# Supercontinuum Generation in a Highly Nonlinear Chalcogenide/ $MgF_2$ Hybrid Photonic Crystal Fiber

**Mahmood Seifouri* and Mohammad Reza Alizadeh**

**Faculty of Electrical Engineering, Shahid Rajaee Teacher Training University, Tehran, Iran**
***Corresponding author:** mahmood.seifouri@srttu.edu

**Received: Jul. 1, 2016, Revised: Oct. 6, 2016, Accepted: Jan. 8, 2017, Available Online: Oct. 28, 2017**

**ABSTRACT— In this paper, we report the numerical analysis of a photonic crystal fiber (PCF) for generating an efficient supercontinuum medium. For our computational studies, the core of the proposed structure is made up of $As_2Se_3$ and the cladding structure consists of an inner ring of holes made up $As_2Se_3$ and four outer rings of air holes in $MgF_2$. The proposed structure provides excellent nonlinear coefficient and dispersion optimization. For the analysis, finite difference frequency domain (FDFD) method is employed. Because of the high nonlinear refractive index of the chalcogenide glass and high difference between the refractive index of the core and the cladding, a small effective mode area of 0.68 $\mu m^2$ is obtained. The nonlinear coefficient is 14.98 $W^{-1}m^{-1}$ at the wavelength of 1.8 µm. Dispersion is almost flat from 1.6 µm up to 2.8 µm. The supercontinuum spectrum calculated ranges from 1 µm to 6 µm. The presented structure is appropriate for medical imaging, optical coherence tomography and optical communications.**

**KEYWORDS:** Supercontinuum generation (SCG), chalcogenide glass, nonlinear effects, photonic crystal fiber, dispersion.

## I. INTRODUCTION

The generation of supercontinuum spectrum has been focused by researchers in recent years due to its wide range of applications in various areas [1-9]. These applications include the use of this spectrum in medical imaging, tomography, metrology, sensors and optical communications [10-12]. PCFs are widely used nowadays due to their flexibility in controlling various optical parameters such as dispersion and nonlinear response [13, 14]. Other advantage of this type of fiber is that a short length of it is required to produce supercontinuum spectrum [15]. One of the important points about PCFs is the controlling of zero dispersion wavelengths (ZDWs). As a result, according to their zero-dispersion wavelength properties, PCFs can be classified into fibers with all normal dispersion and having no ZDW, with single ZDW or with two or more ZDWs [16, 17]. In PCFs with no ZDW, the generation of supercontinuum spectrum is due to self-phase modulation which results in symmetrical broadening of the spectrum on either side of the injected pulse. Although in this case, the produced spectrum is flat but its width is relatively small. In the case of PCFs with single ZDW, the input pulse is injected in the anomalous dispersion region, and the soliton dynamics become important in the generation of supercontinuum spectrum [15, 16].

In PCFs with two zero dispersion wavelengths, the generated output spectrum is much wider than the previously mentioned ones. In this type of PCF, two dispersed waves are produced due to self-phase modulation (SPM) and soliton self-frequency shift process [18, 19]. It should be noted that in this type of PCF, the spectrum has less stability compared to the very first case but its width is much larger. To produce a very flat and broad supercontinuum, a PCF is needed that has both high nonlinear coefficient and flat dispersion profile [20]. In order to increase nonlinear coefficient, either a material with high nonlinear coefficient should be used or effective area should be acceptably small [21, 22].

Many papers have been published on photonic crystal fibers with high nonlinear coefficient. For example, PCFs with different air holes sizes [23], PCFs with small pitch and large air holes sizes [24], structures with equal air holes [25], structures with hybrid cladding [26]. However, these fibers have nonlinear coefficient lower than 80 $W^{-1}$ $km^{-1}$ at the wavelength of 1.55 μm. Using materials with high nonlinear coefficient for the core, one can improve nonlinearity, but however in this case, the dispersion profile is not flat. As a result, designing of PCF with high nonlinear coefficient and flat dispersion is a challenge [27]. In this paper, a PCF with chalcogenide core and the cladding structure consists of an inner ring of holes made up $As_2Se_3$ and four outer rings of air holes in $MgF_2$ is proposed. In this case, because of the high nonlinear refractive index of the chalcogenide glass and also high difference between the refractive index of the core and the cladding, a small effective mode area can be obtained.

This paper is formed as follows. In Section 2, problem formulation is described. Section 3 focuses on the geometry of the proposed PCF. In Section 4, simulation results obtained are presented and discussed and finally the conclusions are presented in Section 5.

## II. PROBLEM FORMULATION

In this paper, dispersion, effective area of the propagating mode, nonlinear coefficient and SCG are fully analyzed and simulated. In this section, the above parameters are discussed and analyzed mathematically.

### A. *Numerical Model*

For numerical simulations of the electromagnetic waves, two dimensional finite difference frequency domains (2D-FDFD) are used [28]. Using perfectly matched layer (PML) conditions, Maxwell's equations are expressed as follows [29-31]:

$$\nabla \times \mathbf{H} = jk_0 s \varepsilon_r \mathbf{E}$$
$$\nabla \times \mathbf{E} = -jk_0 s \mu_r \mathbf{H} \quad (1)$$

where $k_0$, **E**, **H,** $\varepsilon_r$, and $\mu_r$ are the free space wave number, electric and magnetic field, the relative permeability and permittivity constants, respectively. The parameter *s* is the propagation matrix, which is defined as follows [32]:

$$\begin{bmatrix} \frac{s_y}{s_x} & 0 & 0 \\ 0 & \frac{s_x}{s_y} & 0 \\ 0 & 0 & s_x s_y \end{bmatrix} \quad (2)$$

In the above equation, $S_x$ and $S_y$ parameters are obtained by Eq. (3) [30, 32]:

$$s_x = 1 - \frac{\sigma_x}{j\varpi\varepsilon_0}, \text{ and } s_y = 1 - \frac{\sigma_y}{j\varpi\varepsilon_0} \quad (3)$$

where $\sigma$ represents the conductivity of the waveguide and $\varepsilon_0$ is permeability of free space. Finally by using the methods used in [29-32], one can obtain the following equations.

$$\begin{bmatrix} Q_{xx} & Q_{xy} \\ Q_{yx} & Q_{yy} \end{bmatrix} \begin{bmatrix} H_x \\ H_y \end{bmatrix} = \beta^2 \begin{bmatrix} H_x \\ H_y \end{bmatrix} \quad (4)$$

and

$$\begin{bmatrix} P_{xx} & P_{xy} \\ P_{yx} & P_{yy} \end{bmatrix} \begin{bmatrix} E_x \\ E_y \end{bmatrix} = \beta^2 \begin{bmatrix} E_x \\ E_y \end{bmatrix} \quad (5)$$

where $\beta$ is the propagation constant, P and Q are real sparse matrices [34, 35]. For designing the hybrid, PCF proposed in this paper, the following procedure is performed. In the first step, important fiber parameters such as the number of rings, the shape and the size of the holes, the distance between the adjacent holes (Λ) and the materials used, are properly selected. Then for an acceptable accuracy, the mesh size is determined. Then by calculating the propagation constant (β) for the propagating mode, the effective refractive index, $n_{eff}$, can be obtained through Eq. (6).

Finally, the optical parameters of the proposed PCF and SCG are computed [35].

$$n_{FSM} < n_{eff} = \frac{\beta}{k_0} < n_{co} \tag{6}$$

where $n_{eff}$ is effective refractive index, $n_{co}$ is the refractive index of the core, and $n_{FSM}$ is the average refractive index of the clad. Based on calculation of $n_{eff}$, dispersion can be computed by Eq. (7) [36, 37].

$$D(Y) = -\frac{\lambda}{c}\frac{d^2 n_{eff}}{d\lambda^2} \tag{7}$$

In this equation, $\lambda$ is the central wavelength of injected pulse and c is the speed of light in free space.

### B. *SCG Equations*

To investigate SCG, numerical solution of general nonlinear Schrödinger equation (GNLSE) with the split-step Fourier method is used. Simplified form of this equation is as follows [36]:

$$\frac{\partial A}{\partial z} = \left(\hat{D} + \hat{N}\right)A \tag{8}$$

where $\hat{D}$ and $\hat{N}$ represent the linear and nonlinear parts of GNLSE, respectively. These parameters are defined as follows:

$$D = -\frac{\alpha(\omega)}{2} + \sum_{n\rangle 2}\beta_n \frac{i^{n+1}}{n!}\frac{\partial^n}{\partial t^n} \tag{9}$$

and

$$N = i\gamma\left(1 + \frac{i}{\omega_0}\frac{\partial}{\partial t}\right) \int_{-\infty}^{\infty} R(T')\left|A(Z, T-T')\right|^2 dT' \tag{10}$$

In Eq. (9), $\alpha$ is the total fiber loss that is negligible due to a very small length of PCF, R(T) is the response function including the Raman and Kerr nonlinearities. $\beta_n$ represents the nth order dispersion parameter obtained by the following equations[36, 37].

$$\beta_m = \left(\frac{d^m \beta}{d\omega^m}\right)_{\omega=\omega_0} \quad \text{(m=0, 1, 2, …)} \tag{11}$$

and

$$D(\lambda) = -\frac{2\pi c}{\lambda^2}\beta_2 \tag{12}$$

In Eq. (10), $\gamma$ is the nonlinear coefficient obtained from the Eq. (13).

$$\gamma = \frac{\omega_0 n_2(\omega_0)}{cA_{eff}} \tag{13}$$

where $n_2$ is the nonlinear coefficient and $\omega_0$ is the central frequency and $A_{eff}$ is the effective area which is obtained as follows [36, 37]:

$$A_{eff} = \frac{\left(\iint_s |E_t|^2 dxdy\right)^2}{\iint_s |E_t|^4 dxdy} \tag{14}$$

## III. GEOMETRY OF THE PROPOSED PCF

Nowadays with the improvement of the fabrication technology, many complex structures, such as chalcogenide-tellurite composite structures and chalcogenide/silica hybrid structures have been reported in order to achieve the desired dispersion and nonlinear characteristics [38-40]. PCFs with silica core have low nonlinear coefficient. With regard to Eq. (13), to increase nonlinear coefficient, material with higher nonlinear coefficient should be used or the effective mode area should be reduced, or both cases can be used. Here a PCF with chalcogenide/ $MgF_2$ Hybrid structure is used. As the refractive index of chalcogenide glass is much higher than that of $MgF_2$ glass, hence a large difference between the core and the cladding refractive indexes is achieved. As a result, the effective mode area of the proposed structure decreases and its nonlinear coefficient increases.

The linear refractive index dependent on the wavelength of $As_2Se_3$ and $MgF_2$ is obtained by the following equation:

$$n^2(\lambda) = 1 + \sum_{i=1}^{m} \frac{A_i \lambda^2}{\lambda^2 - \lambda_i^2} \qquad (15)$$

where $\lambda$ indicates the wavelength in micrometers. The following table shows values of indices $A_1$, $A_2$, $A_3$, $\lambda_1$, $\lambda_2$ and $\lambda_3$ for $As_2Se_3$ and $MgF_2$ [41-42].

Table 1 Sellmeier fitting coefficients.

| Material | $As_2Se_3$ | | $MgF_2$ | |
|---|---|---|---|---|
| | $A_i$ | $\lambda_i$ (μm) | $A_i$ | $\lambda_i$ (μm) |
| $i$=1 | 0.24164 | 0.24164 | 0.48755708 | 0.04338400 |
| $i$=2 | 0.347441 | 19 | 0.39875031 | 0.09461442 |
| $i$=3 | 1.308575 | 0.48328 | 2.31203530 | 23.7936040 |

Figure1 shows the proposed structure. To create a flat dispersion based on Eq. (7), the first inner ring is selected to be made up of chalcogenide glass with smaller hole diameter than that of other holes in the cladding structure. In Fig. 1, $d_c$, $d_1$, $d$, and $\Lambda$ are the core diameter, chalcogenide inner ring hole diameter, cladding air holes diameter, and the distance between the adjacent air holes (pitch) respectively.

## IV. Simulation Results

To achieve an optimum structure, dispersion profile is calculated for different core and hole sizes. Figure 2 illustrates the dispersion profile for various core sizes. When the core diameter is larger than 1.08 μm, dispersion in the anomalous dispersion region becomes very high. A reduction in the core diameter decreases the dispersion, and when the core diameter is lower than 0.9 μm, dispersion becomes negative. By further decrease in the core diameter, high negative dispersion is achieved. However, the dispersion profile becomes desirable when the core diameter is 0.99 μm.

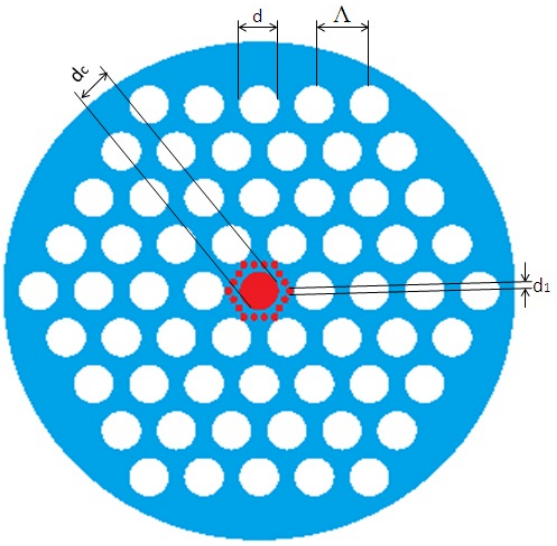


Fig. 1. The structure of the proposed PCF with $As_2S_3$ core and the cladding structure consists of an inner ring of holes made up $As_2S_3$ and four outer rings of air holes in $MgF_2$.

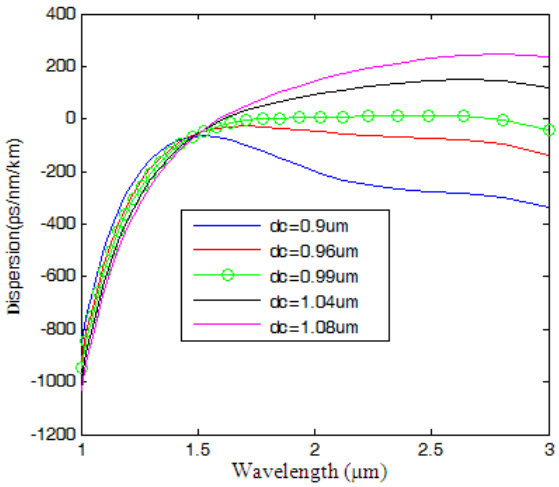


Fig. 2: Effect of the core diameter on dispersion profile.

To create a flat dispersion profile, a chalcogenide ring of holes is introduced immediately around the core. The effect of this set of holes is shown in Fig. 3. In the case of the absence of this ring of chalcogenide holes or even when the diameter of these holes are small, anomalous dispersion increases and the profile is not flat. When $d_1$ is larger than 0.24 μm, the slope of dispersion at shorter wavelengths and in the normal dispersion region decreases and the slope of dispersion at

the longer wavelengths in the anomalous dispersion region increases.

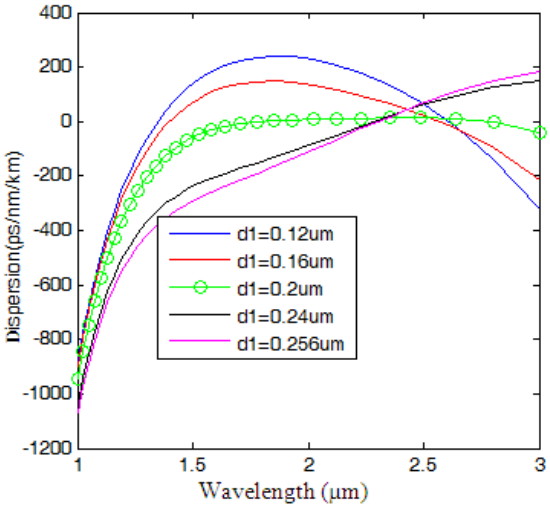


Fig. 3. Effect of Chalcogenide holes diameter on dispersion profile.

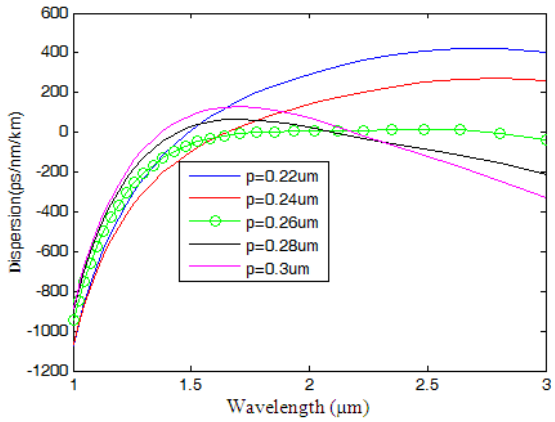


Fig. 4. Effect of Chalcogenide holes, Λ on dispersion profile.

Figure 4 illustrates the effect of variation of Λ of the chalcogenide holes. Reduction of Λ increases the distance between two adjacent ZDWs and increases dispersion in the anomalous dispersion region. Further increase of Λ also increases the normal dispersion and increases the slope of the dispersion. Another important factor affecting the dispersion is the Λ of the cladding air holes. Figure 5 shows the impact of changes in *d* and its Λ on the dispersion profile.

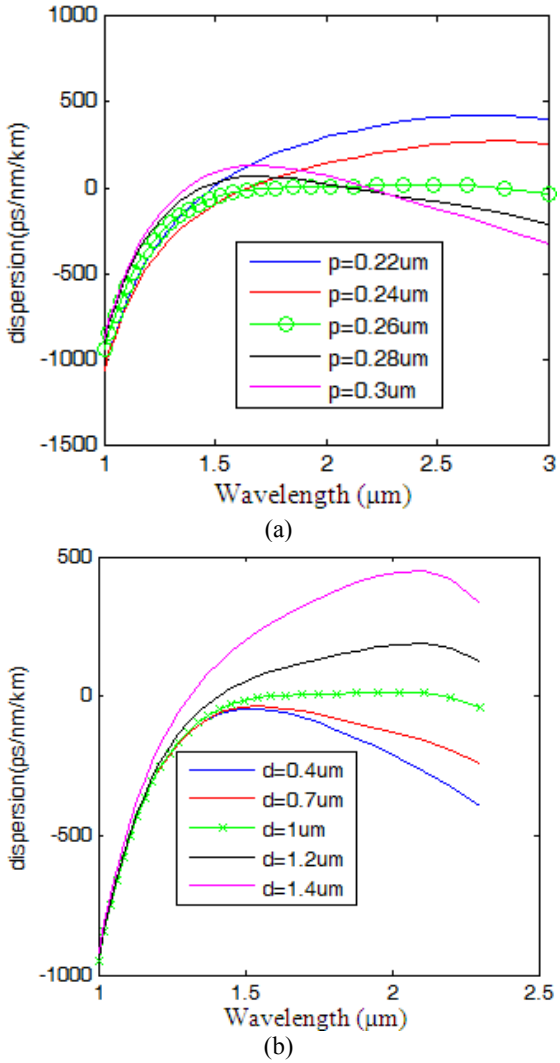


Fig. 5: The effect of changes (a) distance between air holes, Λ and (b) the diameter of the air holes, d on dispersion profile.

In Fig. 5 (a), by reducing Λ, the distance between the two ZDWs increases, and by increasing Λ, the distance between them decreases but in this case the slope of the dispersion increases. In Fig. 5 (b), by increasing d, dispersion in the anomalous dispersion region is increased, but when d is small, the dispersion moves toward normal dispersion region but the slope of the dispersion increases. However, this is not appropriate for supercontinuum generation. Finally, based on the above results, the core diameter is selected to be $d_c$=0.99 μm, the Λ for the chalcogenide holes is chosen to be equal to 0.26μm, the chalcogenide holes

diameter is taken to be $d_1$=0.2 μm, the Λ for the air holes is chosen to be equal to 0.26μm.

With these chosen values, the resulting dispersion profile has 2 ZDWs, one at approximately 1.75 μm and the other at about 2.8 μm.

The effective mode area at the wavelength of 1.8 μm is $A_{eff}$=0.68μm$^2$. As a result, the nonlinear coefficient in proposed PCF is obtained as $\gamma$=14.98 W$^{-1}$m$^{-1}$ with regard to nonlinear refractive index of $As_2S_3$ which is $n_2$=2.92×10$^{-18}$. Figure 6 shows the calculated spectrum evolution in 10 cm propagation length of the proposed PCF. In this case, the input pulse duration is 50fs at the fundamental quasi-TE mode where its power is 200w at the central wavelength of 1.8 μm. It is seen that after about 2 cm, spectrum reaches to relative stability and it is quite stable for 8 cm. Different orders of β are given in Table 2.

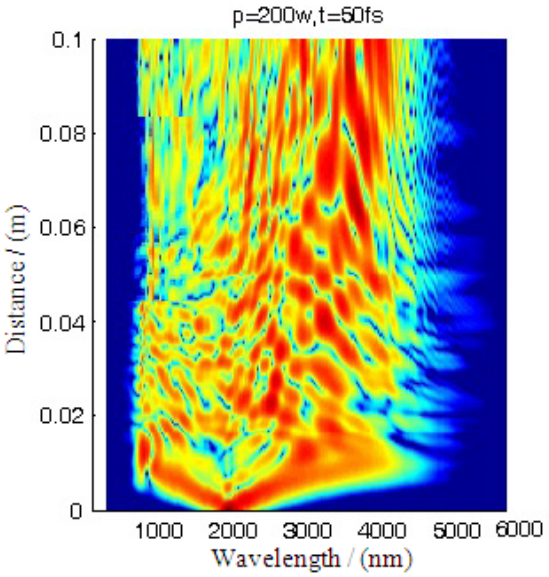


Fig.6: Evolution of the spectral distribution of optical pulses in the proposed PCF with a length of 10 cm.

In Fig. 7, the supercontinuum spectrum obtained by an input pulse width of 32 ps, power of 200 W and fiber length of 10 cm is illustrated.

Figure 8 shows the output supercontinuum spectrum for pumping with the same input pulse but this time with duration of 50 fs.

Figure 9 illustrates the supercontinuum spectrum for the same input pulse but this time with a power of 200 W.

Table 2. The $\beta_n$ parameters of the proposed PCF at the wavelength of 1.8 μm

| $\beta_n$ | Values [ps$^n$/km] |
|---|---|
| $\beta_2$ | -3.7 |
| $\beta_3$ | 0.15 |
| $\beta_4$ | 0.0012 |
| $\beta_5$ | 1.09×10$^{-5}$ |
| $\beta_6$ | -1.35×10$^{-7}$ |
| $\beta_7$ | -1.085×10$^{-10}$ |
| $\beta_8$ | 1.94×10$^{-11}$ |
| $\beta_9$ | -1.518×10$^{-12}$ |
| $\beta_{10}$ | -7.18×10$^{-14}$ |

The generated supercontinuums shown in the figures above have approximate coherence property over the entire bandwidth of 1–6 μm.

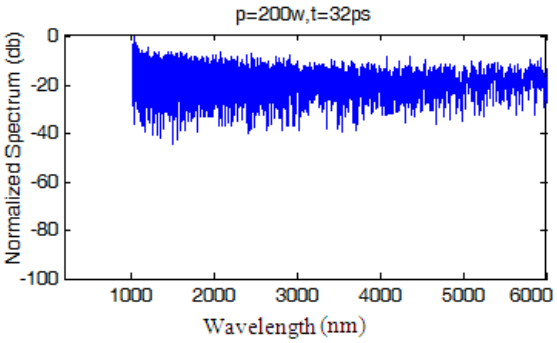


Fig. 7. Supercontinuum spectrum with an input power of 200 W and pulse duration of 32 ps.

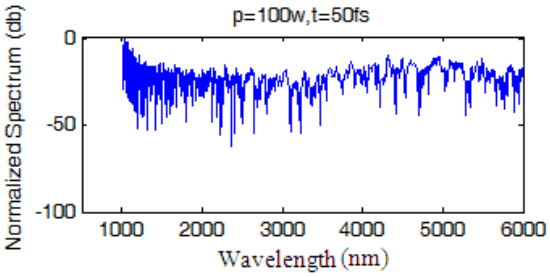


Fig. 8. supercontinuum spectrum with an input power of 100 W and a pulse width of 50 fs.

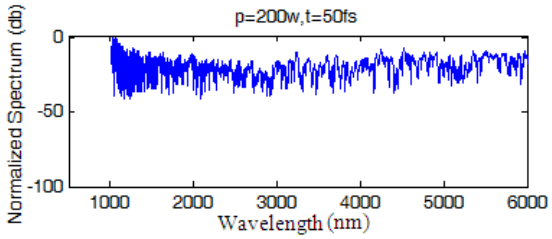


Fig. 9. Supercontinuum spectrum with an input power of 200 W and a pulse width 50 fs.

## V. CONCLUSION

In this paper, the propagation constant and the effective mode area in the proposed PCF are first calculated and then dispersion and supercontinuum spectrum are computed. The proposed structure is made up of $As_2S_3$ and the cladding structure consists of an inner ring of holes made up $As_2S_3$ and four outer rings of air holes in $MgF_2$. Because of the high nonlinear refractive index of the chalcogenide glass and also high difference between the refractive index of the core and the cladding, a small effective mode area of 0.68 $\mu m^2$ and nonlinear coefficient $\gamma$=14.98 $W^{-1}$ $m^{-1}$ are obtained. Dispersion is almost flat from 1.6 μm up to 2.8 μm. The supercontinuum spectrum calculated ranges from 1 μm to 6 μm. This structure is appropriate for medical imaging, optical coherence tomography and optical telecommunications.

## REFERENCES

**[1]** G.A. Nowak, J. Kim, and M.N. Isla, "Stable supercontinuum generation in short lengths of conventional dispersion-shifted fiber," J. Appl. Opt. Vol. 38, pp. 7364-7369, 1999.

**[2]** J.M. Dudley, G. Genty, and S. Coen, "Supercontinuum generation is photonic crystal fiber," J. Rev. Mod. Phys. Vol. 78, pp. 1135-1184, 2006.

**[3]** S. Hideyuki "2-4 Supercontinuum Generation and its Applications," J. National Institute Information Commun. Technol. Vol. 53, pp. 33-40, 2006.

**[4]** J. Bethge, A. Husakou, F. Mitschke, F. Noack, U. Griebner, G. Steinmeyer, and J. Herrmann, "Two-octave supercontinuum generation in a water-filled photonic crystal fiber," Opt. Express, Vol. 18, pp. 6230-6240, 2010.

**[5]** A.M. Heidt, A. Hartung, G.W. Bosman, P. Krok, E.G. Rohwer, H. Schwoerer, and H. Bartelt, "Thulium- doped fiber amplifier for optical communications at 2 μm," Opt. Express, Vol. 19, pp. 3775-3787, 2011.

**[6]** C. Milián and D.V. Skryabin, "Soliton families and resonant radiation in a micro-ring resonator near zero group-velocity dispersion," Optics Express, Vol. 28, pp. 3732-3739, 2013.

**[7]** H.H. Tu and S.A. Boppart, "Laser Photon Coherent fiber supercontinuum for biophotonics," Laser Photon. Rev. Vol. 7, pp. 628–645, 2013.

**[8]** S. Dupont and P.M. Moselund, "Lasse Leick, Jacob Ramsay, Søren R Keiding, Up-conversion of a megahertz mid-IR supercontinuum," J. Opt. Soc. Am. B, Vol. 30, pp. 2570-2575, 2013.

**[9]** B.A. Cumberland, J.C. Travers, S.V. Popov, and J.R. Taylor, "29 W High power CW supercontinuum source," Opt. Express, Vol. 16, pp. 5954-5962, 2008.

**[10]** I. Hartl, X. D. Li, C. Chudoba, R. K. Ghanta, T. H. Ko, J. G. Fujimoto, J. K. Ranka, and R. S. Windeler, "Ultrahigh- resolution optical coherence tomography using continuum generation in an air-silica microstructure optical fiber," Opt. Lett. Vol. 26, pp. 608–610, 2001.

**[11]** H. Kano and H-o. Hamaguchi, "Characterization of a supercontinuum generated from a photonic crystal fiber and its application to coherent Raman spectroscopy," Opt. Lett. Vol. 28, pp. 2360–2362, 2003.

**[12]** K. Mori, K. Sato, H. Takara, and T. Ohara, "Supercontinuum lightwave source generating 50 GHz spaced optical ITU grid seamlessly over S-, C- and L-bands," Electron. Lett. Vol. 39, pp. 544–546, 2003.

**[13]** J. Broeng, D. Mogilevstev, S.E. Barkou, and A. Bjakle, "Photonic crystal fibers, a newclass of optical waveguides," Opt. Fiber Technol, Vol. 5, pp. 305–330, 1999.

**[14]** Ph.St.J. Russell, "Photonic-crystal fibers," J. Lightw. Technol. Vol. 24, pp. 4729–4749, 2006.

**[15]** J.M. Dudley and J.R. Taylor, *Supercontinuum generation in optical fibers*, Cambridge, 2010.

**[16]** L. Tian, L. Wei, and F. Guoying, "Numerical simulation of supercontinuum generation in liquid-filled photonic crystal fibers with a normal flat dispersion profile," Opt. Commun. Vol. 334, pp. 196-202, 2014.

**[17]** A. Hartung, A.M. Heidt, and H. Bartelt, "Design of all-normal dispersion microstructured optical fibers for pulse-preserving supercontinuum generation," Opt. Express, Vol. 19, pp 7742-7749, 2011.

**[18]** M. Michalska and J. Swiderski, "Three-octave spanning supercontinuum generation in a fluoride (ZBLAN) fiber," Electron Technology Conference, Vol. 8902, pp. 89021-89026, 2013.

**[19]** H. Mikami, M. Shiozawa, M. Shirai, and K. Watanabe, "Compact light source for ultrabroadband coherent anti-Stoke Raman scattering (CARS) microscopy," Opt. Express, Vol. 23, pp. 2872-2878, 2015.

**[20]** V. Pureur and J.M. Dudley, "Design of solid core photonic bandgap fibers for visible supercontinuum generation," Opt. Commun. Vol. 284, pp. 1661–1668, 2011.

**[21]** N.S. Shahabuddin, N.A. Awang, H. Ahmad, H. Arof, K. Dimyati, Z. Yusoff, and S.W. Harun, "Supercontinuum generation using a passive mode-locked stretched-pulse bismuth-based erbium-doped fiber laser," Opt. Laser Technol. Vol. 44, pp. 741–743, 2012.

**[22]** K.R. Khan, M.F. Mahmood, and A. Biswas, "Coherent Super Continuum Generation in Photonic Crystal Fibers at Visible and Near Infrared Wavelengths," IEEE J. Selec. Top. Quantum Electron. Vol. 20, pp. 573-581, 2014.

**[23]** Y.M. Wang, X. Zhang, X.M. Ren, L. Zheng, X.L. Liu, and Y.Q. Huang, "Design and analysis of a dispersion flattened and highly nonlinear photonic crystal fiber with ultralow confinement loss," Appl. Opt. Vol. 49, pp. 292–297, 2010.

**[24]** F. Poli, A. Cucinotta, S. Selleri, and A.H. Bouk, "Tailoring of flattened dispersion in highly nonlinear photonic crystal fiber," IEEE Photon. Technol. Lett. Vol, 164, pp. 1065–1067, 2004.

**[25]** V. Finazzi, T.M. Monro, and D.J. Richardson, "Small-core silica holey fibers, Nonlinearity and confinement loss trade-offs," J. Opt. Soc. Am. B, Vol. 20, pp. 1427–1436, 2003.

**[26]** J.F. Liao, J.Q. Sun, Y. Qin, and M.D. Du, "Ultra-flattened chromatic dispersion and highly nonlinear photonic crystal fibers with ultralow confinement loss employing hybrid cladding," Opt. Fiber Technol. Vol. 19, pp. 468–475, 2013.

**[27]** J. Liao, J. Sun, M. Du, and Y. Qin, "Highly Nonlinear Dispersion Flattened Slotted Spiral Photonic Crystal Fibers," IEEE Photon. Technol. Lett. Vol. 26, pp. 380-383, 2014.

**[28]** M.-L. Zhai, W.-Y. Yin, Z (D). Chen, H. Nie and X-H. Wang, "Modeling of ultra-wideband indoor channels with the modified leapfrog ADI-FDTD method," Int. J. Numer. Model. Vol. 28, pp. 50–64, 2015.

**[29]** F.E. Seraji and F. Asghari, "Determination of Refractive Index and Confinement Losses in Photonic Crystal Fibers Using FDFD Method: A Comparative Analysis," Int. J. Opt. Photon. Vol. 3, pp. 3-10, 2009.

**[30]** Z. Zhu and T. G. Brown, "Full-vectorial finite-difference analysis of microstructure optical fibers," Opt. Express, Vol. 10, pp. 853–864, 2002.

**[31]** M. Chen, Q. Yang, T. Li, M. Chen, and N. He, "New high negative dispersion photonic crystal fiber," Optik, Vol. 121, pp. 867–871, 2010.

**[32]** M. Aliramezani and Sh. Mohammad Nejad, "Numerical analysis and optimization of a dual-concentric-core photonic crystal fiber for broadband dispersion compensation," Opt. Laser Techno., Vol. 42, pp. 1209–1217, 2010.

**[33]** Sh. Guo, F. Wu, S. Albin, and R.S. Rogowski, "Photonic band gap analysis using finite-difference frequency-domain method," Opt. Express, Vol. 12, pp. 1741–1746, 2004.

**[34]** S.K. Singh, D.K. Singh, and P. Mahto, "Numerical Analysis of Dispersion and Endlessly Single Mode Property of a Modified Photonic Crystal Fiber Structure," Adv. Network. Appl. Vol. 3, pp. 1116-1120, 2011.

**[35]** T. Karpisz, B. Salski, A. Szumska, M. Klimczak, and R. Buczynski, "FDTD analysis of modal dispersive propertiesof nonlinear photonic crystal fibers," Opt Quant Electron. Vol. 47, pp. 99–106, 2015.

**[36]** G.P. Agrawal, *Nonlinear Fiber Optics*, Academic Press, 2013.

**[37]** G.P. Agrawal, "Nonlinear fiber optics: its history and recent progress," J. Opt. Soc. Am. B, Vol. 28, pp. A1-A10, 2011.

**[38]** M. Liao, X. Yan, G. Qin, C. Chaudhari, T. Suzuki, and Y. Ohishi, "Controlling the chromatic dispersion of soft glass highly nonlinear fiber through complex microstructure," J. Non-Crystalline Solids, Vol. 356, pp. 2613–2617, 2010.

**[39]** C. Chaudhari, M. Liao, T. Suzuki, and Y. Ohishi, "Chalcogenide Core Tellurite Cladding Composite Microstructured Fiber for Nonlinear Applications," J. Lightwave Technol., Vol. 30, pp. 2069-2076, 2012.

**[40]** X. Feng, F. Poletti, A. Camerlingo, F. Parmigiani, P. Petropoulos, P. Horak, G. M. Ponzo, M. Petrovich, J. Shi, W. H. Loh, and D. J. Richardson, "Dispersion controlled highly nonlinear fibers for all-optical processing at telecoms wavelengths," J. Opt. Fib. Technol. Vol. 16, pp. 378-391, 2010.

**[41]** M.R. Karim and B.M.A. Rahman "Ultra-broadband mid-infrared supercontinuum generation using chalcogenide rib waveguide," Opt. Quantum Electron. Vol. 48, pp. 174 (1-10), 2016.

**[42]** R. Cherif, A.B. Salem, M. Zghal, P. Besnard, Th. Chartier, L. Brilland, and J. Troles "Highly nonlinear $As_2Se_3$-based chalcogenide photonic crystal fiber for midinfrared supercontinuum generation," Opt. Eng. Vol. 49, pp. 095002 (1-6), 2010.

**Mahmood Seifouri** received the B.Sc. (Hons) and PhD degrees in electrical and electronic engineering from the University of Wales College of Cardiff, UK, in 1985 and 1989, respectively.

After spending two years as a Lecturer at Brighton University, UK, Dr Seifouri moved to Iran University of Science and Technology in 1991. After spending 9 years at IUST, in 2000, he was employed as a Senior Development Engineer at Bookham Technology, UK, where he was primarily involved in research & development projects in the field of optoelectronics. In September 2001, he joined Optinetrics, CA, USA, as a Senior Development Engineer and continued with his work over there. Since 2006, Dr Seifouri has been with the Faculty of Electrical Engineering, Shahid Rajaee Teacher Training University, Tehran, Iran. His research interests include experimental and numerical studies of electromagnetic fields and waves with particular emphasis on the theory, modeling and simulation of optical waveguides, lasers, amplifiers and nano-scale photonic circuits.

**Mohammad Reza Alizadeh** was born in 1980 in Iran. He received the B.Sc. degree from University of Shamsipur in 2010. He is currently working towards his MSc degree in Electrical and Electronic Engineering at Shahid Rajaee Teacher Training University, Tehran, Iran. His research interests include SCG in PCFs and waveguides and nano-scale photonic circuits.

**THIS PAGE IS INTENTIONALLY LEFT BLANK.**